Resistivity and Hall effect of metallic oxygen-deficient $YBa_2Cu_3O_x$ films in the normal state

B. Wuyts, V. V. Moshchalkov, and Y. Bruynseraede
Laboratorium voor Vaste-Stoffysica en Magnetisme, Katholieke Universiteit Leuven, Celestijnenlaan 200 D, B-3001 Leuven, Belgium
(Received 26 January 1995; revised manuscript received 30 October 1995)

We present a systematic study of normal-state transport properties in a series of *c*-axis-oriented $YBa_2Cu_3O_x$ (YBCO) epitaxial thin films and $YBa_2Cu_3O_7/PrBa_2Cu_3O_7$ (YBCO/PrBCO) superlattices. The hole doping level in the YBCO films is varied from the optimum-doped metallic down to the underdoped insulating regime by changes in the oxygen content x. We find that the magnitude of the resistivity ρ and Hall coefficient R_H increases monotonically with decreasing x and that their respective temperature dependences undergo marked changes. The $R_H(T)$ behavior is reminescent of the Hall effect behavior in heavy fermion metals, taking into account a difference in temperature by a factor of 100. The Hall angle $\cot\theta_H=\rho/R_HB$ shows a quadraticlike temperature dependence, with systematic deviations at high and low doping levels. Transport measurements in YBCO/PrBCO superlattices, with the YBCO layers in the two-dimensional regime, indicate that the deviations of a T^2 dependence of the Hall angle are intrinsic and not related to the dimensionality of the system. A method of analyzing the transport data is presented, revealing a striking scaling behavior of the respective properties. A comparison with reported transport data in the literature suggests that the observed scaling behavior may be universal for underdoped cuprates. Furthermore, we show that reported NMR Knight shift data for oxygen-deficient YBCO samples can also be mapped on a single scaling curve, by using the same scaling parameter derived from our transport measurements. This finding strongly indicates that the dominant scattering mechanism in these materials is of magnetic origin. Going one step further, we present a qualitative analysis of the conductivity under the assumption that we may use the expression for a two-dimensional quantum liquid and that the inelastic scattering length may be replaced by the magnetic correlation length $\xi(T)$. Expressions for the latter are taken from reported calculations for undoped and doped cuprates. A good qualitative agreement is obtained between the calculated and experimentally observed temperature-dependent conductivity.

I. INTRODUCTION

One of the important issues which remains unsolved in physics of the high-temperature superconductors (HTSC's) is the nature of the characteristic excitations in the normal state ($T>T_c$). Many normal-state properties have been found to behave anomalously with respect to a simple metallic or Fermi liquid behavior,[1–3] possibly indicating the existence of quite exotic elementary excitations typical for strongly correlated electron systems. It is commonly accepted now that an insight in the normal state may provide an important clue to the understanding of the superconductivity mechanism itself.[4]

Today, the investigation of the normal state involves a wide variety of electrical, magnetic, and optical studies. Ironically enough, it is the appearance of superconductivity itself at high temperatures which inhibits a proper study of the normal state down to sufficiently low temperatures. Therefore it is of interest to study the normal-state properties in underdoped (lower-T_c) materials. Moreover, systematic studies of the normal-state properties *as a function of doping* from the insulator side up to the high-temperature superconductor side may reveal some interesting insights concerning the evolution of the exotic metallic state from the antiferromagnetic insulating state.

Quite important in this respect is the study of the electrical transport properties as a function of doping. The anomalous temperature dependences of the resistivity ρ and the Hall coefficient R_H, which seem to be a fingerprint of the HTSC's,[1,2] remain difficult to explain. Moreover, the available experimental data seem to indicate that both $\rho(T)$ and $R_H(T)$ depend delicately on the doping level.[5–10] Since these properties are intimately related to the scattering mechanism of the charge carriers, a clear insight in their behaviour is highly desirable.

In the present paper we will first present the results of a systematic study of the normal-state transport properties of $YBa_2Cu_3O_x$ (YBCO) epitaxial thin films as a function of the oxygen content x. Part of these results has appeared already elsewhere.[5,6] The results for $\rho(T)$ and $R_H(T)$ will be described, together with an analysis in terms of the Hall angle $\cot\theta_H$. A quadraticlike temperature dependence is obtained for all oxygen content values, but systematic deviations seem to question the universality of the T^2 dependence of $\cot\theta_H$.

In Sec. IV we will present a method of analyzing the resistivity and Hall effect data.[7] It will be shown that the changes induced by a diminishing hole doping level in the behavior of $\rho(T)$, $R_H(T)$, and $\cot\theta_H(T)$ can be understood as the result of a changing temperature (or energy) scale. For all the studied properties it will be demonstrated that the obtained data can be *scaled onto universal* curves. The scaling parameter T_0, determined from the resistivity data, is the temperature below which ρ is no longer linear in T. A comparison of these striking observations will be made with transport data reported for underdoped YBCO single crystals and for other cuprates. Both seem to corroborate the universality of our scaling observations.

Finally, we will compare the transport data with measurements of magnetic normal-state properties. During the last few years, magnetic measurements like inelastic neutron

scattering or nuclear magnetic resonance have indicated the importance of magnetic spin fluctuations in HTSC's.[11,12] It is well known that the superconducting cuprates become antiferromagnetic (AF) insulators with a Néel transition temperature T_N of several hundred kelvin when the doping level is strongly reduced. The long-range AF order is, however, suppressed with increasing doping, resulting in a vanishing T_N near the insulator-metal transition. Nevertheless, there is nowadays considerable evidence for the existence of *short-range* AF correlations in samples which are well inside the metallic regime (and are superconducting at low temperatures). Moreover, the magnetic measurements clearly indicate that at a temperature well above T_c the spin correlations become very important, resulting in the opening of a *spin gap* in the spin excitation spectrum.[11]

We will present evidence for a remarkable resemblance between the characteristic features found in transport and magnetic properties. This correlation strongly indicates the magnetic origin of the dominant charge carrier scattering mechanism in the cuprates. In view of this finding we will in a last part calculate the conductivity σ in a two-dimensional (2D) quantum antiferromagnet,[13] using the magnetic correlation length ξ as the inelastic scattering length. Several theoretical predictions and calculations of $\xi(T)$ will be considered for the calculation of $\sigma(T)$ and compared to the experimental results.

II. EXPERIMENTAL METHOD

The c-axis-oriented epitaxial thin YBCO films with a thickness of 1000–1100 Å were grown on MgO (100) substrates by a single target 90° off-axis magnetron sputtering technique.[14] X-ray diffraction characterization shows that the as-prepared films are c-axis oriented and of single-phase character. The narrow rocking curve widths ($\Delta\omega_{(005)} \leqslant 0.3°$) indicate a low degree of mosaic spread, while the low ion channeling yields ($\chi_{\min} \leqslant 7\%$) and a detailed transmission electron microscopy study provide evidence for the epitaxial character of the films. The as-prepared films have a high critical temperature ($T_c \simeq 89$ K), a small normal-to-superconducting transition width ($\Delta T_c < 2$ K), and a high critical current density ($J_c \simeq 10^7$ A/cm^2 at $T=5$ K, $J_c \simeq 10^6$ A/cm^2 at $T=77$ K), comparable to the best values quoted in the literature. Patterning of the films into a (2×10) mm^2 structure, necessary for Hall effect measurements, is done by classical photolitographic and wet-etching techniques, without deterioration of the film properties.

The oxygen depletion is carried out *ex situ* using a special heat treatment procedure reported previously.[15] The film is packed in a box of YBCO bulk material and placed inside a quartz tube. The desired nominal oxygen concentration x_n is obtained by a controlled heat treatment of the film following a constant oxygen content (x_n) line in the oxygen-pressure–temperature (P_{O_2}-T) phase diagram of YBCO.[16] This technique has been shown to be reproducible and reversible for the preparation of oxygen-deficient YBCO samples. Although we are not able to measure the *real* oxygen content x of the films in a direct way, we have made an indirect determination by comparing the obtained critical temperatures $T_c(x_n)$ with the $T_c(x)$ behavior observed in YBCO bulk samples,[18] of which the oxygen content is accurately determined by chemical and thermogravimetric analyses. It was found in this way that the nominal oxygen content values x_n are systematically *overestimated by an amount* ~ 0.1. We believe that this effect is related to the particular P_{O_2}-T phase diagram which we have applied for the oxygen reduction process, since we observed recently[19] that the T_c data of YBCO thin films and ceramics collapse when the films are heat treated following the phase diagram of Tetenbaum *et al.*[20] For the sake of consistency, however, all oxygen reduction processes of YBCO thin films in the present study are carried out using the phase diagram of Gallagher.[16] In order to facilitate a comparison of the present results with other available data, the oxygen content values x that we refer to in this work correspond to the original nominal values x_n subtracted by an amount 0.1: $x = x_n - 0.1$. To the fully oxidized films we assign the value for optimum hole doping, $x=6.95$. We estimate the error on the absolute oxygen content value determined in this way to be ~ 0.05.

The temperature dependences of the resistivity and Hall coefficient are measured inside a temperature-stabilized He flow cryostat, using a four-point ac lock-in technique, with a current density $J \leqslant 10^2$ A/cm^2. All electrical contacts are made by direct wire bonding onto the film surface using AlSi wires. The Hall coefficient is obtained from the transverse voltage between two opposing contacts, measured using a classical field inversion technique, in a magnetic field $B=0.72$ T. For all the films the Hall voltage varies linearly with applied field and current.

III. RESULTS

A. Resistivity

Using the method described above, we have systematically varied the oxygen content in several c-axis-oriented YBCO films and measured the temperature dependence of the resistivity. Figure 1 shows a compilation of $\rho(T)$ data from three different films. Although for several of the indicated x values the $\rho(T)$ behavior was measured in more than one film, we show for clarity only one curve per x value. Note that the upper temperature window was always restricted to $\simeq 300$ K since we observed a time-dependent behavior of ρ above 300 K, which we believe is caused by rearrangement of oxygen in the CuO-chain plane.[17]

It is clear from Fig. 1 that the reduction of the oxygen content leads to a corresponding decrease of T_c as is well known for YBCO. Another important consequence of the oxygen reduction in the YBCO films is the marked increase in absolute resistivity. Starting from a value $\rho(290\ \text{K}) \simeq 300$ $\mu\Omega$ cm for $x=6.95$, it increases to $\rho(290\ \text{K}) \simeq 4$ mΩ cm for $x=6.3$ as shown in Fig. 2. Although there is some scatter in the data, both due to an uncertainty in x and in the exact film thickness t, a clear trend emerges. With decreasing x the resistivity goes up smoothly at first, but at $x=6.5$, the curve suddenly increases much faster. This kink may be related to the sudden change in carrier concentration n which is seen in many calculations for $n(x)$ (Refs. 21–23) around this x value.

According to Fig. 1, the $\rho(T)$ curve for $x=6.95$ shows the well-known linear temperature dependence, as discussed in the Introduction. However, reducing x below its optimum doping value produces a clear change in the temperature de-

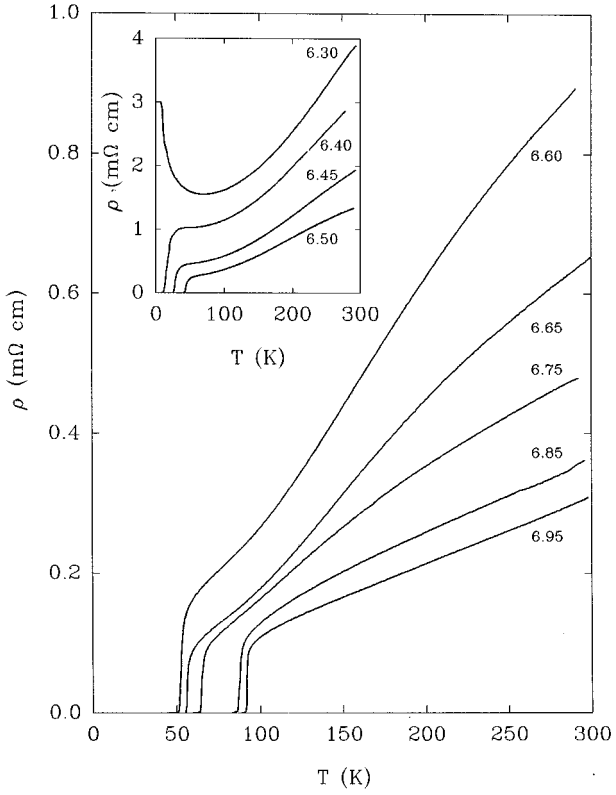

FIG. 1. Resistivity ρ vs temperature T as a function of the oxygen content x in c-axis-oriented YBCO films. The results are obtained from YBCO No. 1 ($x=6.95$, 6.85, 6.75, 6.65), YBCO No. 2 ($x=6.6$, 6.5, 6.45, 6.4), and YBCO No. 5 ($x=6.3$).

pendence of ρ.[5,6] The temperature interval in which ρ is linear systematically shifts to higher temperatures, and a downward bending develops at lower temperatures, eventually followed by an upward bending becoming more pronounced for the lowest x values. Finally, for the nonsuperconducting $x=6.3$ sample, we observe only the upward bending, indicating the onset of localization effects.

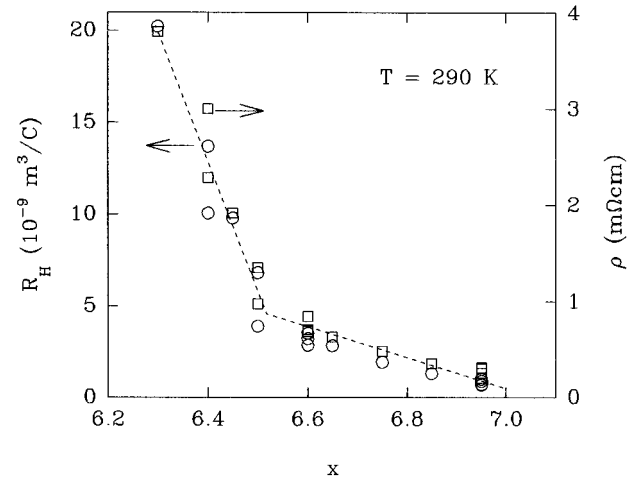

FIG. 2. Variation of the resistivity ρ(290 K) (left scale, squares) and of the Hall coefficient R_H(290 K) (right scale, circles) with oxygen content x in the YBCO films. The dashed line is a guide to the eye.

A similar change in temperature dependence, including the development of a kind of ''S shape,'' has been reported also for oxygen-deficient YBCO single crystals[8,24] and thin films,[25–27] for Co-doped YBCO single crystals,[9] and also for underdoped $La_{2-y}Sr_yCuO_4$ (LSCO) ceramics[28] and single crystals.[29] On the other hand, several studies on Zn-doped[30] or Pr-doped YBCO single crystals[31] show a linear T dependence of ρ also in samples with reduced critical temperatures. The difference between both classes of systems, showing a nonlinear respectively linear $\rho(T)$ behavior in samples with reduced T_c's, is the mechanism which suppresses superconductivity, i.e., electron doping versus disorder.

Hence the following consistent picture seems to emerge: A pronounced nonlinear $\rho(T)$ behavior develops systematically in cuprates with reduced hole densities, while a linear behavior with constant slope but increased magnitude of ρ is obtained in cuprates in which T_c is suppressed by other means than hole doping (e.g., by disorder).

B. Hall effect

For the same samples on which we measured the resistivity and in the same measuring run, we have studied the behavior of the Hall number $n_H(T)=1/[R_H(T)e]$. The main result of $n_H(T)$ as a function of x is shown in Fig. 3 for nine different oxygen concentration values (from the same samples as used for Fig. 1). We preferred to show the data for the different oxygen content films in separate graphs, since plotting them all together may be misleading. In the following we will focus on the relation of R_H with the carrier density and on the changes of the temperature dependence with varying x.

Note that the Hall effect behavior in the vicinity of T_c, i.e., in the ''mixed state,'' is mainly governed by the movement of magnetic flux lines. This regime will not be treated here since it goes beyond the scope of the present work (see, e.g., Ref. 32).

Although the pronounced temperature dependence of R_H makes it too arbitrary to extract absolute values for the carrier density n, it is nevertheless interesting to look at the relative changes in R_H with oxygen doping in YBCO. Therefore we have plotted in Fig. 2 besides the resistivity values also the values of R_H at $T=290$ K versus the oxygen content x for all the measured samples.

The figure shows the same trend for the Hall coefficient data than for the resistivity data: Starting from the optimum doping value $x=6.95$, R_H increases monotonically with decreasing x, displaying a *kink* at $x\simeq 6.5$, below which the increase in R_H is much faster. This result, which is independent of temperature, is in good agreement with the $R_H(x)$ behavior reported for ceramic YBCO samples[33] which also shows a sharp increase in R_H at $x\simeq 6.5$. Since both R_H and ρ are inversely proportional to the density of mobile carriers n in the CuO_2 planes (at least in a free-electron picture), it is tempting to assign the characteristic x dependence of both properties to the x dependence of n. Furthermore, this idea is supported by the calculated behavior of the hole density versus oxygen content in YBCO,[21–23] showing a sharp drop in n at $x\simeq 6.5$.

Contrary to what some authors claim,[1] the temperature dependence of n_H does not disappear with decreasing hole density, but is pronounced for *all* x values as shown in Fig. 3.

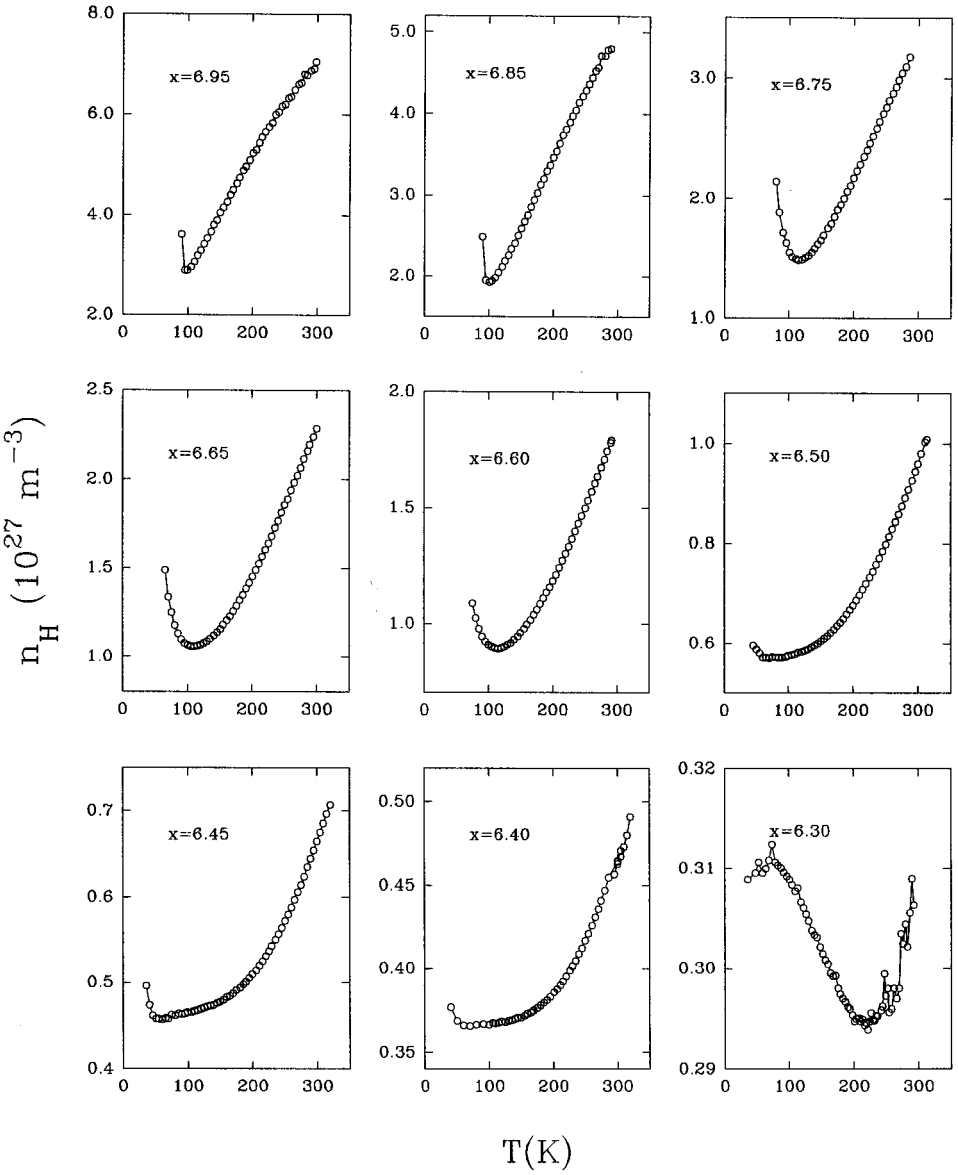

FIG. 3. Hall number $n_H = 1/R_H e$ vs temperature T as a function of the oxygen content x in c-axis-oriented YBCO films. (Some data points at the lowest temperatures have been omitted for clarity.)

Only the *amplitude* of n_H goes down with decreasing x. Furthermore, although the curves might all look very similar at first sight (except for $x=6.3$), a systematic evolution in the temperature dependence is perceptible. For the fully oxidized sample, with $x=6.95$, a T-linear Hall number is obtained in agreement with published data for optimum doped cuprates.[34,35] Linearity is, however, not observed up to the highest temperatures as sometimes reported, but instead the n_H curve tends to bend off for $T>220$ K. This bending disappears for the lower oxygen content values, yielding a linear behavior over almost the whole temperature region from 300 K down to T_c for the $x=6.85$ sample. By further reducing x, it can be seen that a broad minimum develops, and as a consequence, the onset of linearity shifts systematically to a higher temperature. Similarly as in case of the resistivity, this systematic evolution seems to indicate that the reduction of the oxygen content leads in fact to a systematic change of the temperature scale. We will further discuss this interesting finding in Sec. IV.

The characteristic temperature dependence of R_H in the cuprate superconductors was discussed by Fiory and Grader[36] in terms of asymmetric magnetic scattering or ''skew scattering.'' This *extraordinary* Hall effect arises from asymmetric scattering of conduction electrons by local magnetic moments and occurs in addition to the Lorentz force that is responsible for the *ordinary* Hall effect.[37] The skew scattering mechanism was also proposed[38–40] to explain the anomalous Hall effect behavior in the *heavy fermion metals*. As the cuprates, these materials are characterized by strong electron correlations and by the presence of localized magnetic moments (situated on the $4f$ or $5f$ shell) which can be viewed as the counterpart for the $3d$ moments in the cuprates. These moments, being independent at high temperatures, form so-called ''Kondo singlets'' below the Kondo temperature T_K and become coherent below a temperature $T_{\rm coh}<T_K<10$ K (below which Fermi liquid behavior is established). For the Hall coefficient, this results in a characteristic temperature dependence: At low T, R_H is almost constant and of modest size, while, as T increases above $T_{\rm coh}$, R_H rapidly rises as a result of the onset of magnetic skew scattering, then reaches a maximum, and monotonically decreases. The similarity with the $R_H(T)$ behavior in

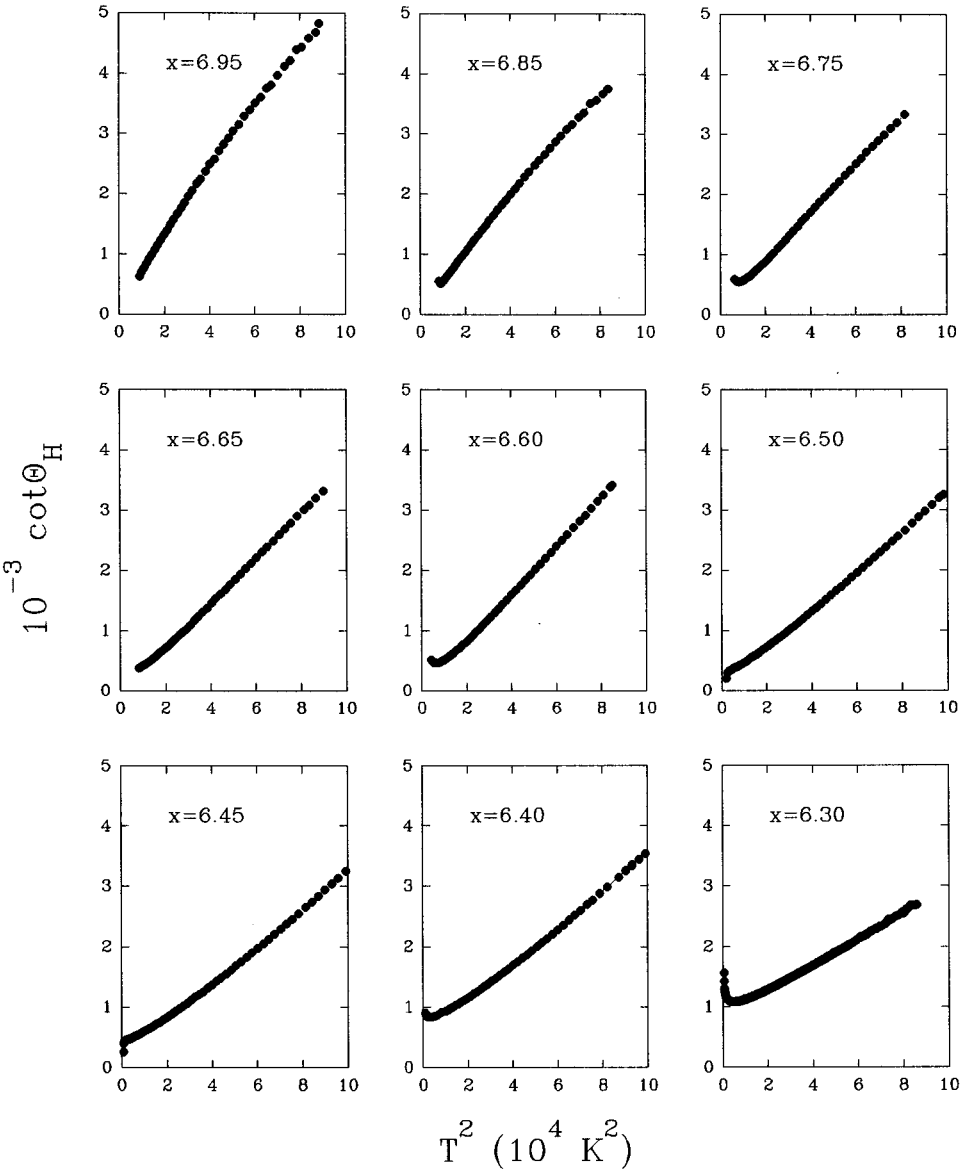

FIG. 4. Cotangent of the Hall angle $\cot\theta_H$ vs the square of the temperature, T^2, calculated from the resistivity and Hall coefficient data shown in Figs. 1 and 3.

the cuprates, as first pointed out by Fiory and Grader,[36] makes it attractive to invoke the same physical mechanism in both classes of materials. This would lead to a ''coherency temperature'' $T_{\rm coh}$ for the cuprates which is higher by a factor of 100 compared to the values for the heavy fermion metals.[3] Note that the typical superconducting transition temperatures in high-T_c and heavy fermion superconductors differ also roughly by the same factor.

In order to check the plausibility of a skew scattering picture, the field dependence of the Hall voltage can be investigated. Since the anomalous component to the Hall signal saturates when the external magnetic field B exceeds the value required to fully polarize the magnetic moments, the total Hall voltage should show a deviation from linearity at high fields. We have checked the field dependence of the Hall voltage for a YBCO thin film with $x=6.7$ at several temperatures and for magnetic fields up to 10 T. The obtained results clearly indicate that the Hall voltage V_H is perfectly linear with the field B up to 10 T. This might be used as an argument against skew scattering in these samples, as is done by several authors.[1,41] However, when we again apply the analogy to the heavy fermion systems, we can estimate the magnetic field necessary to align the magnetic moments from the energy required to destroy the Kondo singlets: $\mu_B B \sim k_B T_K$, with μ_B the Bohr magneton and k_B Boltzmann's constant. Hence, for an estimated Kondo temperature $T_K \simeq 100$ K in the cuprates, a magnetic field $B \simeq 160$ T is required. Very recent results of the Hall voltage in pulsed magnetic fields (up to 40 T) seem to indicate the onset of saturation,[42] thus leaving the skew scattering picture still plausible.

C. Hall angle

In view of the experimental and theoretical findings mentioned in Sec. I, it is interesting to compute the Hall angle from the resistivity and Hall effect data for the series of oxygen-deficient YBCO thin films.[5,6] Figure 4 shows $\cot\theta_H$ versus T^2 calculated from the results presented in Figs. 1 and 3 in the previous sections. It can be seen that irrespective of the complicated temperature dependences of ρ and R_H, a *quadraticlike* temperature dependence of $\cot\theta_H$ is obtained for all x values.

When looking to the linear part in all the curves of Fig. 4, we clearly observe a systematic evolution with varying oxygen content. First, the slope $d(\cot\theta_H)/d(T^2)=\alpha$ decreases systematically with decreasing x, and second the intercept $C=\cot\theta_H(T=0)$ becomes nonzero for $x<6.5$. In former papers we have elaborated these findings[5,6] and presented evidence for a linear relation between the Hall angle slope α and the hole density in the CuO_2 planes n. It was shown that therefore α may be a better measure of the hole density than the Hall number n_H.

Although the quadratic temperature dependence of $\cot\theta_H$ is nowadays often considered as a universal property of the high-T_c cuprates, we would like to point out that some reservation may be necessary. A closer look to the different curves in Fig. 4 reveals that only for the intermediate oxygen concentrations is a linear behavior obtained over the full temperature range. The films with large x clearly show a sublinear behavior, in particular at higher temperatures, while the films with small x demonstrate an upturn of $\cot\theta_H$ at low temperatures.

A careful analysis of published Hall angle data reveals similar trends, although these deviations from perfect T^2 behavior are usually ignored or assigned to extrinsic effects.

Since it is generally known that with reducing x in YBCO also the dimensionality is changed from anisotropic 3D towards 2D, the deviations observed at high doping levels might originate from the non-2D character of the samples. In order to check this possibility, we have carried out some additional $\rho(T)$ and $R_H(T)$ measurements in a set of $YBa_2Cu_3O_7/PrBa_2Cu_3O_7$ (YBCO/PrBCO) superlattices with varying PrBCO layer thicknesses (1:1, 1:3, 1:5).[43] With increasing PrBCO thickness, the dimensionality of the system is artificially lowered, keeping the oxygen content in the YBCO layers constant ($x=6.95$). Hence, if the dimensionality is important for the behavior of the Hall angle, one would expect a systematic evolution of $\cot\theta_H(T^2)$ in this set of samples. The results for the behavior of the Hall angle are shown in Fig. 5. It can be seen in this figure that there is clearly no systematic improvement of the linearity of $\cot\theta_H$ in the more decoupled superlattices (1:3, 1:5), indicating that the deviations are not directly related to the dimensionality of the system.

A careful investigation of the available experimental Hall angle results in the literature indicates that the deviations from a T^2 dependence that we observe for high and low x values are generally observed for YBCO samples with high and low *doping levels*. Therefore we believe that those deviations should not be neglected, but they should rather be included in the theoretical models.

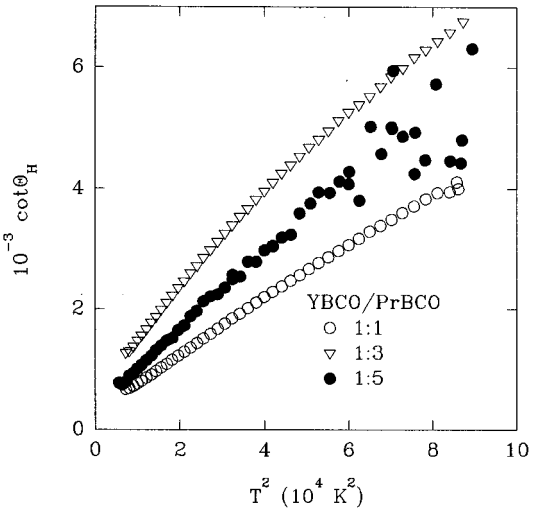

FIG. 5. cot θ_H vs T^2 for three YBCO/PrBCO superlattices, with different layer thicknesses. The YBCO layer is one unit cell thick in all samples, while the PrBCO thickness varies from one up to five unit cells. The larger noise for the 1:5 sample arises from its higher longitudinal resistance compared to the other samples.

IV. DISCUSSION

A. Scaling behavior

From the foregoing it has become clear that although the reduction of the oxygen content in YBCO gives rise to different temperature dependences of the transport properties, the changes take place in a very systematic way.[8] As an example, we refer back to the $\rho(T)$ behavior, where we saw that the T-linear part systematically shifts towards higher temperatures when x is lowered and simultaneously a pronounced S shape develops at lower temperatures. This evolution becomes even more clear when we plot the derivative $d\rho/dT$ versus temperature for the oxygen-deficient YBCO films, as done in Fig. 6. For clarity we have cut off the normal-to-superconducting transitions. It can be seen that a

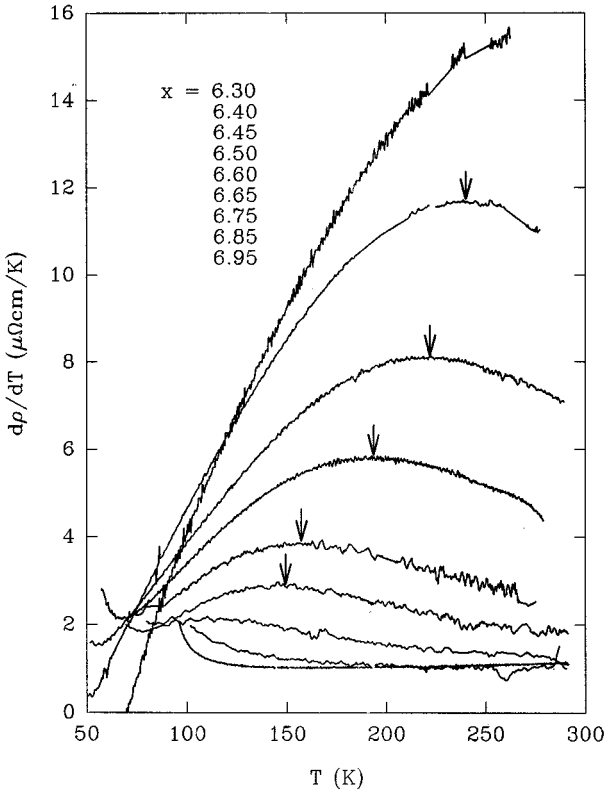

FIG. 6. Temperature derivative of the resistivity $d\rho/dT$ vs temperature T as a function of the oxygen content. The data correspond to the bare $\rho(T)$ curves which were shown in Fig. 1. The arrow indicates the position of the maximum in the curves which appears at a temperature $\sim T_0/2$.

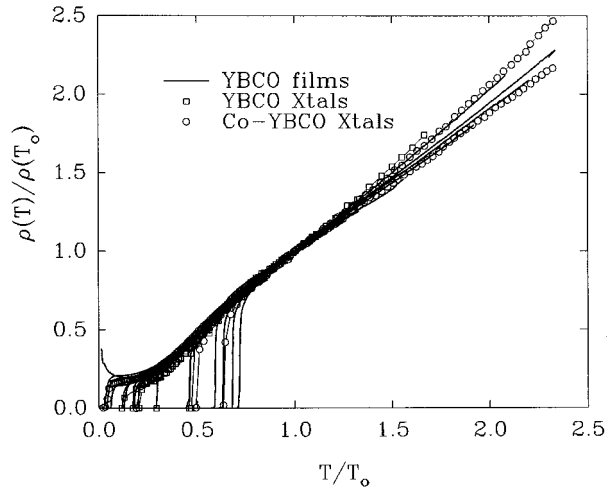

FIG. 7. Scaled in-plane resistivity $\rho/\rho(T_0)$ vs scaled temperature T/T_0 for 15 thin film samples, together with reported data for oxygen-deficient (Ref. 8) and Co-doped (Ref. 9) YBCO single crystals.

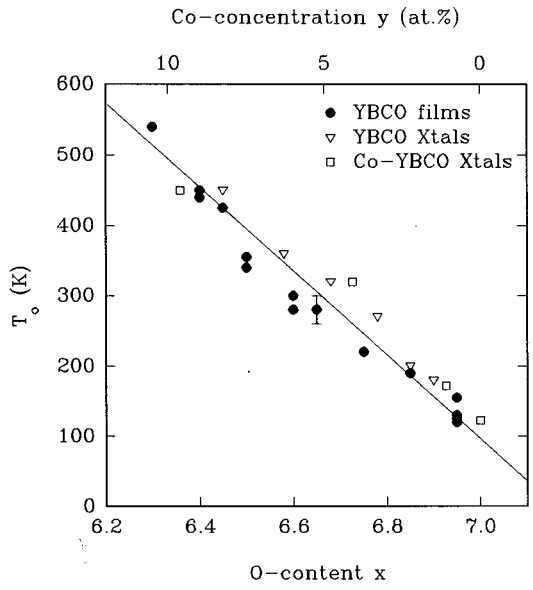

FIG. 8. Characteristic temperature T_0 vs oxygen content x and Co doping level y, for the oxygen-deficient c-axis YBCO films and single crystals (Ref. 8) and for the Co-doped YBCO single crystals (Ref. 9). A typical error bar is indicated; the line is a guide for the eye.

maximum in $d\rho/dT$ (see the arrows in Fig. 6) develops systematically with decreasing x, which simultaneously shifts to higher temperatures.

In order to quantify this evolution, we can define a characteristic temperature T_0 as the temperature above which ρ is linear in T. In Fig. 6, T_0 corresponds to the temperature above which the derivative is constant and is approximately equal to twice the temperature of the maximum in $d\rho/dT$, as may be seen. Hence T_0 can be determined in a direct way for the data sets with $x>6.5$ and can be estimated for the samples with $x\leqslant 6.5$ as twice the temperature of the maximum in the derivative. By deriving T_0 in this way for all measured samples, we estimate that an error of ± 20 K has to be taken into account.

Using the characteristic temperature T_0, we may now scale the temperature axis and simultaneously scale the resistivity with the value of ρ at T_0.[8] The result of this operation for all the available thin film resistivity data (15 data sets in total) is shown in Fig. 7. Very interestingly, we can see in this figure that to a good approximation *all the* $\rho(T)$ *curves collapse onto one universal curve*.[6] Given the considerable overlap in the reduced-temperature scale between the 15 resistivity curves, it is very unlikely that this scaling result is a fortuitous coincidence or an artificial effect of splicing separate curves together.

The universal resistivity curve consists of an S-shaped part for $T/T_0<1$, followed by a linear part for $T/T_0>1$, which approximately extrapolates to zero for $T=0$. Hence this scaling curve clearly demonstrates the limited validity of the often-cited T linearity of the resistivity. Note that the curves tend to separate slightly at $T/T_0>1.5$. This may be due to small differences in residual resistivity between the different samples, which was not included as an extra parameter in the scaling.

In order to check whether the scaling behavior of the resistivity is an intrinsic property of YBCO, we have also applied the same scaling procedure to reported data on oxygen-deficient YBCO *single crystals* ($x=6.45$, 6.58, 6.68, 6.78, 6.85, 6.9) by Ito *et al.*[8] and on *Co-doped* YBCO single crystals (Co doping level $y=0.0\%$, 1.1%, 4.1%, 9.6%) by Carrington *et al.*[9] and included them in Fig. 7. Since Co substitutes Cu in the CuO chains, as was shown by neutron diffraction,[44] it is assumed that Co doping reduces the carrier density.[45] This is in contrast to, e.g., Zn doping, which substitutes Cu in the CuO_2 planes and leads to an increased disorder scattering.[46] Hence a combination of the thin film data with the two studies cited above compares samples of different nature (thin film versus single crystal) and hole doping mechanisms from different origins (O deficiency versus Co doping). It can be clearly observed in Fig. 7 that the scaled data points for the single crystals agree very well with the thin film data. The scaled curves from the oxygen-deficient YBCO single crystals tend to saturate at a slightly smaller low-temperature value, which may be due to a lower residual resistivity of these single crystals.

The fact that the scaling behavior of $\rho(T)$ is observed in different YBCO samples with a variety of hole densities strongly indicates that the main scattering mechanism in YBCO remains unchanged when the carrier concentration is reduced from its optimum value down to the metal-insulator transition.[6,8] The characteristic energy scale on which the scattering occurs and which is determined by the temperature T_0 decreases monotonically with increasing oxygen content or decreasing Co doping level, as shown in Fig. 8. These results therefore confirm the close similarity between oxygen reduction and Co doping to vary the carrier concentration in YBCO. This is in sharp contrast to, e.g., Zn doping, which leaves the overall temperature dependence of the resistivity unchanged, except for a constant term added.[30]

After having demonstrated the scaling behavior of the resistivity, it becomes particularly interesting to make the same kind of analysis for the Hall effect data. Using the *same characteristic temperature* T_0 as for the resistivity, we have

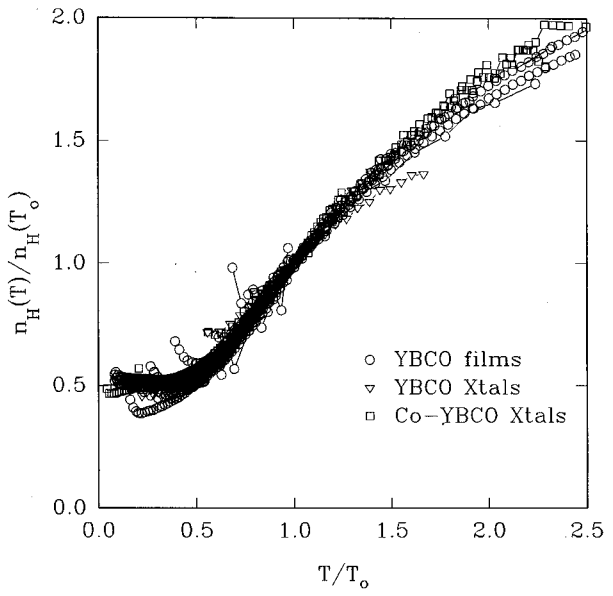

FIG. 9. Hall number n_H divided by $n_H(T_0)$ vs reduced temperature T/T_0 for 15 sets of thin film data together with reported data for oxygen-deficient (Ref. 8) and Co-doped (Ref. 9) YBCO single crystals.

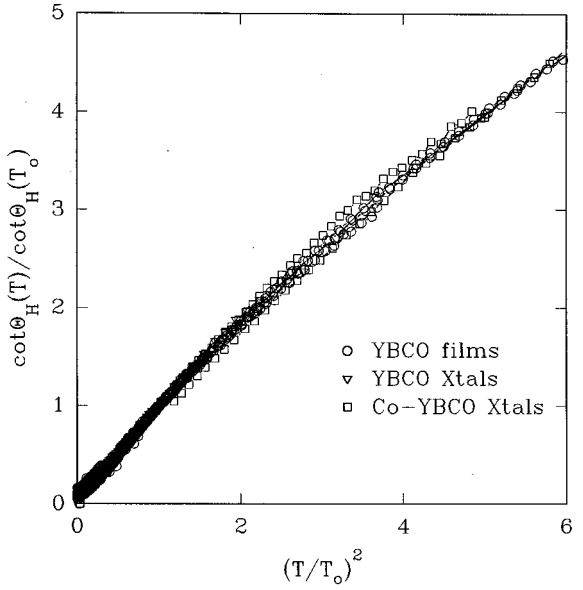

FIG. 10. Cotangent of the Hall angle $\cot\theta_H$ divided by $\cot\theta_H(T_0)$ vs the square of the reduced temperature $(T/T_0)^2$, for 15 sets of thin film data together with reported data for oxygen-deficient (Ref. 8) and Co-doped (Ref. 9) YBCO single crystals.

plotted in Fig. 9 the Hall number versus temperature scaled with $n_H(T_0)$ and T_0, respectively. Included are the 15 sets of thin film data together with the reported data on oxygen-deficient[8] and Co-doped[9] YBCO single crystals. It can be seen that within the experimental scatter on the data again one universal Hall number versus temperature curve emerges. This behavior follows an S-like shape which is approximately linear in only a very limited temperature region $0.75<T/T_0<1.25$. At higher temperatures the curve bends off, tending towards a saturation, while at lower temperature the scaling curve levels off more sharply at $T/T_0\simeq 0.5$ to a constant value. The inflection point of the transition from a positive to a negative curvature occurs exactly at the characteristic temperature T_0.

The observation of scaling behavior for the Hall number, using the same scaling parameter as the one derived from the resistivity data, is quite surprising. It strongly indicates that both properties are governed by the same characteristic energy.

In view of the scaling observations for the separate resistivity and Hall effect data, a scaling behavior is expected to appear also for the Hall angle $\cot\theta_H=\rho/R_H.B$. Again, using the same scaling parameter T_0 derived from the resistivity data, we plot in Fig. 10 the scaled cotangent of the Hall angle, $\cot\theta_H/\cot\theta_H(T_0)$, versus the square of the reduced temperature, $(T/T_0)^2$, for the 15 sets of thin film data and the reported data on oxygen-deficient[8] and Co-doped[9] YBCO single crystals. As expected, all the data are mapped onto a single curve.

Figure 10 clearly shows that the often-cited quadratic temperature dependence of $\cot\theta_H$ is only valid in a limited low-temperature region $[0.3\leqslant(T/T_0)^2\leqslant 1.5]$. At a higher reduced temperature a good fit to the data is obtained using the relation $\cot\theta_H=\alpha' T^p+C'$ with $p=1.69$. The latter value is in good agreement with $p=1.63$ reported by Hofmann *et al.*[47] for nearly optimum doped YBCO thin films.

B. Comparison with magnetic measurements

In order to get more insight into the meaning of the characteristic temperature T_0, we will compare in this section the *electrical* transport results with published data on normal-state *magnetic* properties. There exists nowadays growing evidence for the intimate relation between magnetic and transport properties,[8,48,49] which may be the clue to the understanding of HTSC.[50]

In the past few years, a very intensive effort has been developed to study the spin excitations in HTSC's using inelastic neutron scattering (INS). An excellent review of the measurements carried out in YBCO as a function of hole doping is provided by Rossat-Mignod *et al.*[11] While the INS research was initially concentrated on the antiferromagnetic state in the undoped parent compounds $YBa_2Cu_3O_6$ and La_2CuO_4, interesting results have more recently also been obtained for the metallic compounds. In particular, the INS measurements show that although the long-range AF order is destroyed above a certain doping value ($x\simeq 6.4$ in YBCO), dynamical short-range AF correlations persist also in metallic samples ($x>6.4$ in YBCO). Furthermore, it was found that in underdoped YBCO samples a so-called *spin gap* or *pseudogap* opens up in the spin excitation spectrum at a temperature T_{SG}, well above the superconducting transition temperature T_c, below which the spins become highly correlated [analog of the coherent state in the heavy fermion metals at $T<T_{coh}$ (Ref. 51)].

The opening of a spin gap has also been confirmed by NMR measurements of the Knight shift ΔK and of the spin-lattice relaxation time (T_1). The Knight shift ΔK expresses the frequency shift of the NMR signal caused by the Pauli susceptibility χ_s of the free-electron band[12] (besides a

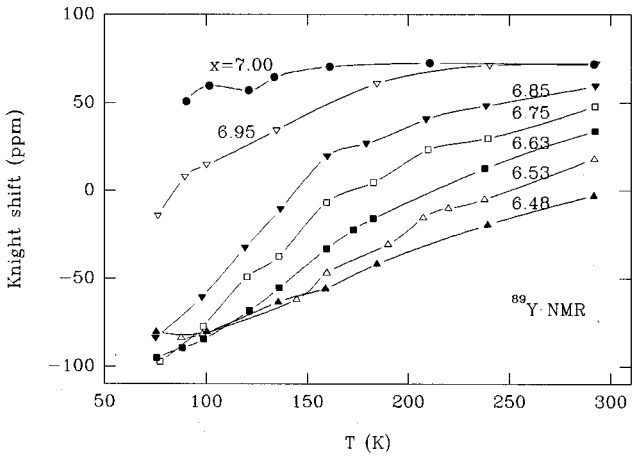

FIG. 11. NMR Knight shift $^{89}\Delta K$ vs temperature T from 77 to 300 K for a series of YBCO samples with different oxygen contents x, after Ref. 52.

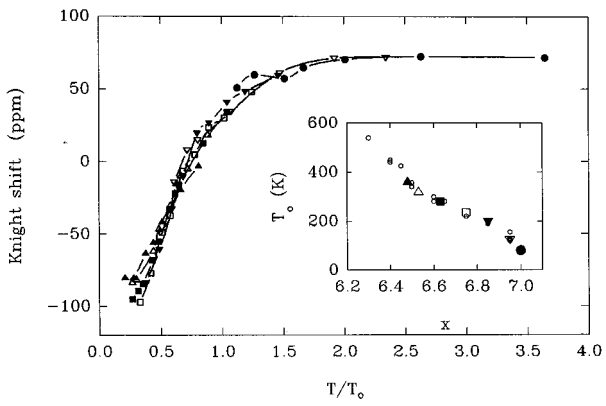

FIG. 12. Knight shift data from Alloul (Ref. 52) for $7 \leqslant x \leqslant 6.48$ plotted vs reduced temperature T/T_0. Inset: characteristic temperature T_0 vs oxygen content x; the small circles represent the values for the YBCO thin films (from transport; cf. earlier) and the larger symbols (same as in main graph) correspond to the NMR samples ($x=7$, 6.95, 6.85, 6.75, 6.63, 6.53, and 6.48).

temperature-independent chemical shift δ) and is usually temperature independent in normal metals.

Figure 11 shows the Knight shift $^{89}\Delta K$ versus temperature reported by Alloul[52] for YBCO samples with varying x. In this case ΔK is measured on the ^{89}Y nuclei, but very similar temperature dependences are obtained at the ^{17}O and ^{63}Cu nuclei.[12,53]

It can be seen in Fig. 11 that while the NMR shift is nearly T independent (Pauli-like) for $x=7$, a large decrease of $|^{89}\Delta K|$ at low T occurs even for slightly depleted samples. This effect is associated with an anomalous reduction of the susceptibility χ_s, due to the increase of AF spin correlations at low T in the spin system or, in other words, due to the opening of the spin gap. The figure clearly shows that with reducing x the decrease in $|^{89}\Delta K|$ starts at systematically higher temperatures, indicating that the spin gap temperature T_{SG} increases with decreasing hole doping.

It was shown before[8] that these Knight shift results closely resemble the behavior of ρ/T versus T. Hence the latter suggests that the spin gap temperature T_{SG} determined by NMR Knight shift measurements may be related to the characteristic temperature T_0 determined from transport measurements.

In order to check this suggestion, we have assigned a characteristic temperature T_0 value to the NMR data ($7 \leqslant x \leqslant 6.48$) using the $T_0(x)$ relation presented in Fig. 8 and replotted the Knight shift data from Alloul,[52] shown in Fig. 11, versus reduced temperature T/T_0. The result of this operation is shown in Fig. 12. Clearly, all the temperature-dependent Knight shift data for the samples with different oxygen contents collapse onto one curve.

This scaling observation shows that also for the magnetic properties the physics does not change with decreasing hole doping, but rather the temperature scale changes. Moreover, the fact that this scaling behavior is obtained using the *same characteristic temperature T_0 derived from transport measurements* (shown in the inset of Fig. 12) strongly indicates that transport and magnetic properties in YBCO are closely related.

Besides the Knight shift, also the temperature dependence of the spin-lattice relaxation rate $(T_1T)^{-1}$ shows specific features which may be related to the effects seen in transport measurements. Unlike the Knight shift, however, the temperature dependence of $(T_1T)^{-1}$ differs for the different probing NMR nuclei. The temperature dependences of $^{17}\mathrm{O}(T_1T)^{-1}$ and $^{89}\mathrm{Y}(T_1T)^{-1}$ closely follow the behavior of $\Delta K(T)$ shown earlier, while $^{63}\mathrm{Cu}(T_1T)^{-1}(T)$ behaves quite differently, showing a broad maximum.[52–54]

Unfortunately, there are too few $^{63}\mathrm{Cu}(T_1T)^{-1}(T)$ relaxation rate data in underdoped YBCO samples, so that a comparison with transport data may be rather hazardous. The results for $x \simeq 6.6$ reported by Takigawa *et al.*[53] and Alloul[52] show a broad maximum at $T \simeq 150$ K. In contrast, a sharp maximum in $^{63}\mathrm{Cu}(T_1T)^{-1}(T)$ is always observed for the fully oxidized samples near T_c. Although the broad maximum for $x \simeq 6.6$ shows up at a much lower temperature than its expected characteristic temperature ($T_0 \simeq 300$ K), it may also be connected to the opening of a spin gap.[55]

Given the difference in the spin gap temperature derived from $\Delta K(T)$, $^{17}\mathrm{O}(T_1T)^{-1}(T)$, or $^{89}\mathrm{Y}(T_1T)^{-1}(T)$, on the one hand, and $^{63}\mathrm{Cu}(T_1T)^{-1}(T)$, on the other hand—which seem to differ by a factor of 2—some authors suggest the possibility of a spin gap opening at different temperatures for different locations inside the Brillouin zone.[48] In our opinion, a more extensive study of $^{63}\mathrm{Cu}(T_1T)^{-1}(T)$ as a function of x is required in order to clarify this issue.

C. Comparison with other cuprates

It is interesting to compare the present results with the normal-state properties measured as a function of the hole doping level in other high-T_c cuprates, in particular LSCO. Systematic measurements of the temperature dependence of ρ (Ref. 29) and R_H (Refs. 10,56) in *underdoped* LSCO ($y < 0.15$) samples show the same characteristic features as in case of underdoped YBCO, i.e., an S shape of $\rho(T)$ which becomes more pronounced for lower y values, and a saturation of R_H at low temperatures. This indicates that the transport properties of underdoped LSCO may be described by similar scaling functions as for YBCO.

For *overdoped* LSCO ($y \geqslant 0.15$) ceramics and thin films, Hwang *et al.*[10] recently reported the observation of a scaling of $R_H(T)$. In this study, a characteristic temperature T^* marks the crossover from a pronounced temperature dependent R_H at low temperatures to a temperature-independent R_H at higher temperatures. Our observation of a saturation onset in n_H at high temperatures (see Fig. 9) implies that a similar crossover in the behavior of the Hall coefficient seems to exist in overdoped YBCO. Very recently, the latter has indeed been demonstrated in Ca-doped $SmBa_2Cu_3O_x$ thin films by Chen *et al.*[57] The authors obtained a very similar scaling curve as the one reported by Hwang *et al.*[10] Both characteristic temperatures T_0 and T^*, defined from resistivity and from Hall coefficient data, respectively, show a similar decreasing behavior with increasing hole concentration in the CuO_2 planes.

Hence the comparison with several reported results in the literature indicates that the scaling observations of the transport properties, which we have presented above for underdoped YBCO compounds, can be expanded towards other cuprates and towards a wider doping range covering both underdoped and overdoped regimes. This suggests that the observed scaling behavior is an intrinsic property of the CuO_2 planes.

Also, the magnetic properties have been extensively studied in the normal state of LSCO. Johnston[58] demonstrated the existence of a scaling relation for the macroscopic magnetic susceptibility $\chi(T)$ in LSCO samples with different Sr concentrations. This scaling was later confirmed by Nakano *et al.*[49] using NMR measurements. Moreover, these authors additionally showed the close resemblance between the behavior of $\chi(T)$ and that of $\rho(T)$, for Sr contents between 0 and 0.3 (i.e., underdoped and overdoped regimes).

The characteristic temperatures derived from the magnetic[49] and the Hall effect[10] measurements in LSCO correspond remarkably well to each other, and both increase with decreasing Sr concentration (i.e., with decreasing hole content), similar to our observations for YBCO (see Fig. 8).

Convincing correlations between transport and magnetic measurements have also been reported for $YBa_2Cu_4O_8$ (1:2:4) compounds.[48,59] The 1:2:4 material[60] is closely connected to the YBCO 1:2:3 compound, the former having two CuO (chain) planes per unit cell instead of one for the latter. It is generally believed that the 1:2:4 system is a slightly underdoped cuprate, resulting in a $T_c \simeq 80$ K. It may therefore be compared with slightly oxygen-deficient YBCO samples.

Similarly to the above observations for YBCO 1:2:3, Bucher *et al.*[48] demonstrated that in the 1:2:4 compound a temperature $T_D^* \simeq 160$ K characterizes the downward bending in the resistivity, an inflection point in the Hall coefficient, and the maximum in $^{63}\mathrm{Cu}(T_1T)^{-1}(T)$. Note that the value of 160 K corresponds to the characteristic temperature T_0 for a YBCO sample with $x \simeq 6.85$ (Fig. 8), having approximately the same T_c ($\simeq 80$ K) as that of the 1:2:4 compound.

From this short overview it becomes clear that there exists a close correlation between the electrical transport and the magnetic properties in several HTSC compounds. The results clearly indicate that both type of properties are governed by the same characteristic temperature, which may be related to the opening of a spin gap. Because of the apparent universality of the characteristic temperature, we believe that the latter should be included in the generic phase diagram of the HTSC's, as shown schematically in Fig. 13.

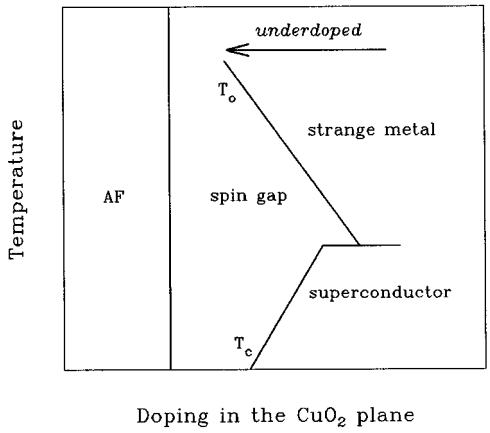

FIG. 13. Schematic drawing of the HTSC phase diagram in the plane of hole doping and temperature, including the characteristic temperature T_0.

D. Theoretical consideration of the spin gap

A quite attractive model to explain the appearance of a spin gap and its dependence upon doping seems to be the resonating-valence-bond (RVB) theory of Nagaosa and Lee.[61] Based on this theory, a general phase diagram for the HTSC's has been obtained, as schematically shown in Fig. 14.[62,55] It can be seen that the underdoped side of the latter is qualitatively very similar to the experimental phase diagram presented in Fig. 13.

In the mean-field approximation of the RVB theory, two characteristic temperatures govern the physics. On the one hand, T_{RVB}, below which the spin degrees of freedom (spinons) form a kind of Zhang-Rice singlets[63] or spin polarons, and on the other hand T_B, below which the charge degrees of freedom (holons) become paired and Bose condense. According to the phase diagram presented in Fig. 14, one can distinguish four different regimes. For $T > T_{\mathrm{RVB}}$ and $T > T_B$, an anomalous metallic state ("strange metal") is ob-

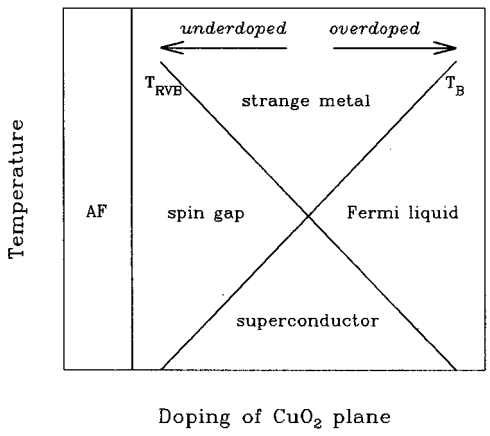

FIG. 14. Shematic presentation of the mean field phase diagram for the CuO_2 plane as proposed by Nagaosa and Lee (Ref. 61).

tained (with, e.g., $\rho \propto T$). At the underdoped side of the diagram, a spin gap state develops between T_{RVB} and T_B. At the overdoped side, a Fermi liquid behavior results below T_B and above T_{RVB}. Finally, for $T<T_{\mathrm{RVB}}$ and $T<T_B$, superconductivity sets in. Although in YBCO only the underdoped regime is probed, there is a good agreement with the theoretically predicted and the experimentally observed behavior, when the characteristic temperature T_0 is identified with the temperature for singlet pairing, T_{RVB}.

The microscopic magnetic scattering mechanism of the charge carriers is still debated. Following the predictions of Nagaosa and Lee,[61] the charge carriers can be scattered by the spin system in two different ways. On the one hand, they can be scattered by chiral spin excitations, which are situated around the origin of the dispersion law of the spin excitations (low **q**) and which can be probed by the NMR Knight shift. On the other hand, the charge carriers can also be scattered by AF spin fluctuations (high **q**), which are well probed by the spin-lattice relaxation rate at ^{63}Cu.

The available experimental data on YBCO indicate that the spin gap temperature of the resistivity (T_0) coincides with the onset temperature of the spin gap in the Knight shift, while the spin gap opening in $^{63}\mathrm{Cu}(T_1T)^{-1}$ apparently occurs at $\sim T_0/2$. Therefore these findings strongly favor the low-**q** scattering mechanism in YBCO.

E. Conductivity in a 2D quantum antiferromagnet

After having convincingly demonstrated the close relation between electrical and magnetic properties, we will in this final section briefly investigate the possibility to explain in a phenomenological way the temperature dependence of the conductivity (i.e., the inversed resistivity). To do this, we will make use of two basic assumptions which we believe are valid in case of the high-T_c cuprates.[13]

(1) We assume that the charge carrier scattering is dominated by magnetic spin fluctuations, so that the inelastic length L_ϕ is given by the magnetic correlation length ξ.

(2) In view of the layered structure of the HTSC's and the pronounced anisotropy of the transport properties, we use the quantum transport expression for σ (Ref. 13) derived for 2D metallic systems by Gor'kov, Larkin, and Khmelnitskii:[64]

$$\sigma \simeq \sigma_{2\mathrm{D}} \propto \ln\left(\frac{L_\phi}{l}\right) \simeq \ln\left(\frac{\xi}{l}\right), \tag{1}$$

with l the elastic mean free path.

In the following paragraphs we will consider some important predictions for the behavior of $\xi(T)$. Using Eq. (1), we can then qualitatively compare the behavior of $\ln \xi(T)$ with the experimentally observed $\sigma(T)$.

1. Correlation length in the undoped compounds

The behavior of $\xi(T)$ for the case of the undoped parent compounds $YBa_2Cu_3O_6$ or La_2CuO_4 has been theoretically described in a paper by Chakraverty, Halperin, and Nelson[65] and for weakly doped compounds by Chubukov, Sachdev, and Ye.[66] These papers are certainly the main reference works in this area. Starting from a 2D $S=1/2$ Heisenberg model on a square lattice—which presents a good description of the undoped cuprates[67]—with nearest-neighbor interactions only, the authors calculate the behavior of the correlation length ξ as a function of temperature in the framework of the quantum nonlinear σ model.[65]

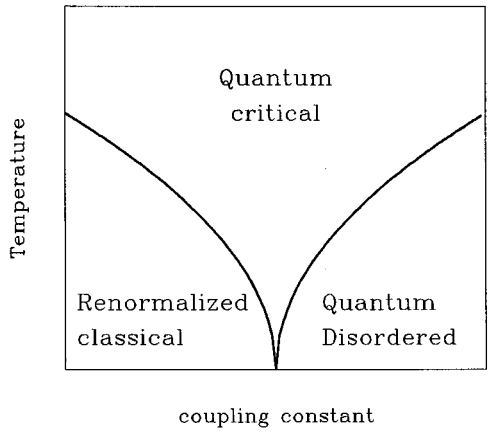

FIG. 15. Schematic representation of the theoretically calculated phase diagram by Chakraverty *et al.* (Ref. 65).

On the basis of the obtained $\xi(T)$ behavior, they can distinguish three separate regions depending on the temperature and the coupling constant (which is inversely proportional to the exchange interaction J). In the *renormalized classical* region an exponential dependence

$$\xi \propto \exp\left(\frac{2\pi\rho_s}{k_BT}\right) \tag{2}$$

is obtained, where ρ_s expresses the spin stiffness ($\propto J$). The main effect of weak doping is to decrease the bare spin stiffness.[66] The *quantum critical* regime is characterized by a magnetic correlation length ξ, which is inversely proportional to T, and in the *quantum disordered* regime, ξ becomes independent of T. The three regimes are schematically presented in Fig. 15.

The results of the calculations by Chakraverty, Halperin, and Nelson[65] and Chubukov, Sachdev, and Ye[66] are in good agreement with results of other calculations and with the experimentally determined $\xi(T)$ behavior for La_2CuO_4.[65,66] However, it remains still unclear whether the results may be extrapolated up to optimum doped compounds, as studied in the present work.

Sokol and Pines[68] have combined the results of Chakraverty *et al.* with NMR data to propose a "unified magnetic phase diagram" for the cuprate superconductors. In essence, they consider the coupling constant in Fig. 15 as the doping level. Roughly speaking, the renomalized classical region then corresponds to the long-range antiferromagnetic Néel phase, the quantum critical region to the anomalous metallic phase, and the quantum disordered region to the spin gap phase. Although this analysis looks attractive, it implies a spin gap temperature which increases with increasing hole doping. Obviously, this is in sharp contrast with the experimental observations.

A rather different picture emerges when we compute $\sigma(T)$ from $\xi(T)$ using Eq. (1). Because of the logarithmic dependence of σ on ξ, one can see immediately that the famous T linearity of the resistivity (or $\sigma \propto \rho_s/T$), which is valid above the characteristic temperature T_0 in YBCO, is obtained when ξ depends exponentially on ρ_s/T.[13] The latter is effectively

the case inside the renormalized classical regime, implying that the high-T_c cuprates with a linear temperature dependence of the resistivity (i.e., optimum and underdoped cuprates) are in the renormalized classical regime for $T>T_0$. Hence, from Fig. 15, it follows that for $T<T_0$ the cuprates should remain inside this regime. Then the question naturally arises: Which effect in $\xi(T)$ causes the change in $\sigma(T)$ at $T=T_0$, if it is not a transition to another regime in the phase diagram?

2. Exchange interaction with a small anisotropy

A possible answer may be provided by a recent paper of Ding.[69] He shows that a 2D AF spin-1/2 Heisenberg system undergoes a transition to an XY system when a small in-plane anisotropy is included in the exchange interaction J. Ding uses this argument to explain the occurrence of long-range magnetic ordering in a 2D system at finite temperatures. The latter is experimentally observed in many systems, including undoped cuprates, but is in contradiction with the theoretical prediction for a pure 2D Heisenberg system.[70,71]

In this paper, Ding considers a 2D AF anisotropic model of the XXZ type which describes the in-plane spin interactions:

$$H=J\sum_{\langle ij\rangle}[S_i^xS_j^x+S_i^yS_j^y+(1-\lambda)S_i^zS_j^z]. \tag{3}$$

The parameter λ describes the anisotropy; the isotropic Heisenberg system is obtained for $\lambda=0$, the pure XY system for $\lambda=1$. Monte Carlo calculations have been carried out using Eq. (3), yielding results for the transverse ($\langle S^yS^y\rangle$) and longitudinal ($\langle S^zS^z\rangle$) spin correlation functions. From the correlation functions at several temperatures, the respective correlation lengths ξ_T and ξ_L and their temperature dependences have been computed. It was found that while the longitudinal correlation length behaves much like in an isotropic spin-1/2 antiferromagnet [cf. Eq. (2)], the behavior of the transverse correlation length is given by the expression for the spin-1/2 XY model,

$$\xi_T\propto\exp\left(\frac{B}{(T-T_c^{XY})^{1/2}}\right). \tag{4}$$

Here $B\propto J$ and T_c^{XY} is the magnetic ordering temperature in the XY system.

It may be seen from Eq. (4) that a small anisotropy in the exchange interaction J results in a magnetic correlation length which no longer diverges at $T=0$, but rather at a finite temperature T_c^{XY}. This indicates that at a temperature $T_{\rm cr}$ above T_c^{XY} the spin system undergoes a crossover from the Heisenberg behavior to the XY behavior. This crossover temperature depends on the anisotropy λ, according to the relation

$$\frac{k_B(T_{\rm cr}-T_c^{XY})}{J}\propto\lambda. \tag{5}$$

The point that we want to focus on here is that a very similar analysis might be applicable for the dynamic spin system in the doped metallic cuprates. If we assume that there is a small anisotropy in the exchange interaction J, a transition from a Heisenberg-like behavior to an XY-like behavior may occur at $T_{\rm cr}$, which we correlate then with the characteristic temperature T_0. Hence the temperature dependence of the magnetic correlation length ξ for $T>T_{\rm cr}$ is given by Eq. (2) and for $T<T_{\rm cr}$ by Eq. (4). By means of Eq. (1), which relates $\xi(T)$ to $\sigma(T)$, we expect that the resistivity will change from $\rho\propto T$ to $\rho\propto(T-T_c^{XY})^{1/2}$.

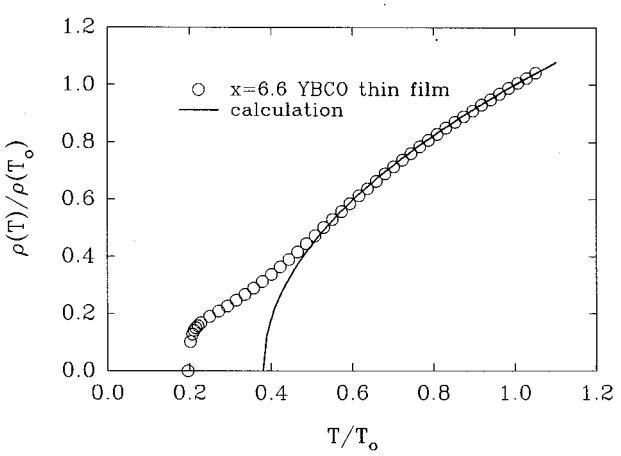

FIG. 16. Scaled resistivity curve for an oxygen-deficient YBCO film with $x=6.60$ (open symbols), together with a calculation of $\rho(T)$ using Eqs. (1) and (4) (line).

In order to check this, we plotted in Fig. 16 the scaled resistivity curve for an YBCO thin film with $x=6.60$ (representative for the universal scaling curve for $T/T_0\leqslant 1$) with a calculation of $\rho(T)$ using Eq. (1) with $\xi(T)$ given by Eq. (4). For this calculation we used $T_c^{XY}=0.38T_0$. It can be seen that a reasonable agreement is obtained between the calculation and the experimental curves for $0.5<T/T_0<1$. Below $T/T_0=0.5$, the resistivity changes its curvature, possibly indicative of the onset of localization.

Because of the scaling behavior, the relation $T_c^{XY}=0.38T_0$ should be valid for all x values. Hence, like T_0, the temperature T_c^{XY} is a decreasing function of x. Intuitively, this might be understood as the consequence of a decreasing anisotropy of J with x, which is consistent with the decreasing anisotropy between the in-plane and out-of-plane directions in YBCO (2D towards 3D behavior), but not consistent with the behavior of the in-plane a-b anisotropy, which increases with decreasing x.

3. Correlation length in doped cuprates

Since the previous calculations are, strictly speaking, only valid for the undoped and weakly doped cuprates, it is of interest to check $\xi(T)$ calculations for relatively large levels of doping. Such studies are, however, not abundantly present in the literature. One particularly interesting work in this area has been reported in the Ph.D. thesis of Reefman.[72] He has presented a Monte Carlo study of a 2D Heisenberg antiferromagnet as a function of doping. As in the previous paragraph, a slightly anisotropic exchange interaction J is adopted. For his study Reefman considers a model of real space pairs (RSP's), moving in an AF background.[73] The RSP's are built up of singlet states which are already paired above the critical temperature T_c (at which the pairs Bose condense).[74,75] The singlet states may, for instance, be

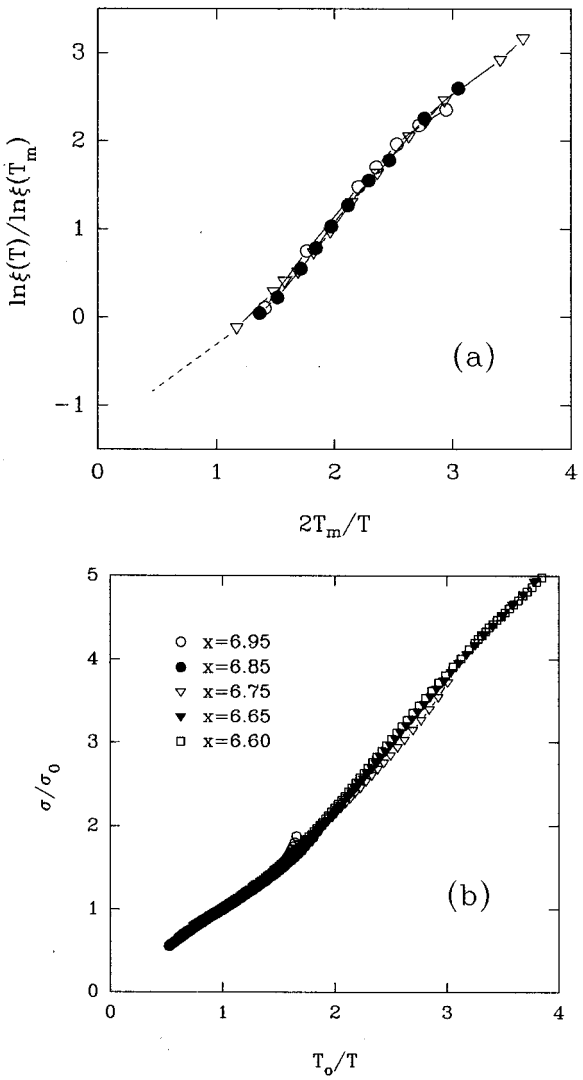

FIG. 17. (a) Scaled ln ξ/ln $\xi(T_m)$ data obtained from Monte Carlo calculations (Ref. 72) for three different carrier concentrations n vs reduced inverse temperature $2T_m/T$; (b) Scaled conductivity σ/σ_0 vs reduced inverse temperature T_0/T for one YBCO film and five different oxygen content values.

viewed as a kind of Zhang-Rice singlets,[63] in which the spin of a doped hole combines with a copper spin to form a singlet, consisting of the copper atom with its four neighboring oxygen atoms.

The results calculated for the NMR Knight shift (i.e., the susceptibility) and spin-lattice relaxation rate $(T_1T)^{-1}$ are in very good agreement with experiments as a function of hole doping. For instance, the broad maximum in $^{63}\mathrm{Cu}(T_1T)^{-1}$ is nicely reproduced and shifts systematically to higher temperatures for lower doping levels, as observed experimentally.

Besides the NMR properties, also the temperature dependence of the magnetic correlation length is calculated for the different doping levels. In order to check for a possible scaling behavior, we have plotted the logarithm of the calculated $\xi(T)$ results for three different carrier densities n versus a reduced inverse temperature $2T_m/T$ in Fig. 17(a). Note that this way of presenting the results enables a direct comparison with the experimental data for $\sigma(T)$ through Eq. (1). T_m represents the temperature of the maximum in the spin-lattice relaxation rate $^{63}\mathrm{Cu}(T_1T)^{-1}$ and is explicitly quoted in the work of Reefman for the different carrier densities.[72] We have reduced the temperature in Fig. 17(a) on purpose by *twice* T_m since the available experimental data on $^{63}\mathrm{Cu}(T_1T)^{-1}(T)$ are indicative for a relation $T_0 \simeq 2T_m$ (cf. supra). The values of lnξ are reduced by the respective values at T_m (ξ at $2T_m$ was not calculated).

Quite astonishingly, the calculated $\xi(T)$ data also show a clear scaling behavior. Moreover, a good qualitative agreement is obtained between the scaled conductivity behavior for the YBCO films, shown in Fig. 17(b), and the lnξ behavior shown in Fig. 17(a) (in which the extrapolation to higher temperatures is indicated by the dashed line). Although the number of data points from the Monte Carlo calculations is rather limited, it may be seen that both data sets show a change of slope around the same reduced inverse temperature and a slight bending at higher inverse temperatures.

Hence these findings—in particular the scaling observation of the calculated $\xi(T)$ behavior—once more support the idea that the electrical conductivity is mainly determined by magnetic scattering in the cuprates. Furthermore, the results may indicate the validity of the real space pairing approach for the normal state.

4. Experimental determination of $\xi(T)$

Finally, some remarks about the experimentally observed $\xi(T)$ behavior for doped cuprates have to be made. Neutron scattering studies on the doped YBCO system indicate that ξ is essentially independent of temperature in a wide temperature range.[11,76] On the other hand, ξ extracted from NMR measurements on YBCO 1:2:4 samples[59] is clearly T dependent and increases with decreasing temperature. As pointed out by Tomeno *et al.*,[59] a comparison between both results is difficult due to the complicated situation to determine ξ from the imaginary part of the dynamic susceptibility, as is done in neutron scattering studies. Hence, in order to check the theoretical predictions for $\xi(T)$ in case of doped cuprates, more reliable experimental data are necessary.

5. Other alternatives: density-of-state peaks and singularities

The linear temperature dependences of the resistivity and Hall number in high-T_c cuprates can be also successfully described by assuming the existence of the narrow density of states $g(E)$ in the vicinity of the Fermi level E_F.[77–79] However, the microscopic origin of the narrow $g(E)$ peak has not been found. It is worth noting here that one of the possible mechanisms leading to the formation of the density-of-states peak, mentioned in Ref. 78, is an appearance of the saddle-point singularity in the vicinity of the Fermi level. The existence of such a van Hove singularity has been recently confirmed in high-resolution angle-resolved photoemission experiments.[80,81] At this moment it is not clear yet whether the narrow density-of-states peak model can also explain the observed evolution of transport properties and the scaling behavior of resistivity, Hall number, and the Knight shift.

V. CONCLUSIONS

In this paper we have presented and discussed experimental normal-state transport data on oxygen-deficient YBCO

films. From the resistivity curves a characteristic temperature T_0 is derived which separates the linear part at high temperature from the S-shaped part at low temperature. By scaling T with T_0 and ρ with $\rho(T_0)$, all the thin film data collapse onto one universal curve. In addition, resistivity data taken from the literature for underdoped YBCO single crystals are mapped on the universal resistivity curve as well. Using the same characteristic temperature T_0, a scaling behavior is also observed for the Hall effect and Hall angle data.

These results indicate that a reduction of the hole doping level in YBCO does not affect the dominant scattering mechanism, but rather modifies the energy scale on which the scattering occurs. Furthermore, the universal scaling curves clearly show that the transport properties obey the often cited linear or quadratic temperature dependences only within limited temperature intervals. Hence theoretical models describing the normal state of the cuprates should not only explain these simple temperature dependences, but rather the full scaling curves as well.

From a comparison of the transport behavior with published data on the magnetic normal-state properties of the cuprates, it becomes clear that both types of properties are governed by the same physics. As the most prominent feature, we note that we have mapped published NMR Knight shift data for oxygen-deficient YBCO onto a single curve by scaling the temperature axis with the *same characteristic temperature T_0 derived from our transport measurements*. These findings indicate that the spin correlations, which are believed to determine the anomalous behavior of the magnetic properties, are also governing the transport properties in the cuprates. It is then most likely that T_0 is related to the opening of a spin gap in the spin excitation spectrum, which is observed in NMR and neutron scattering experiments.

Finally, we have examined some theoretical predictions for the temperature dependence of the magnetic correlation length and tried to correlate them with the behavior of the conductivity in the YBCO films. It follows that the optimum and underdoped YBCO results can be classified within the renormalized classical regime. This is in agreement with underdoped LSCO, which can also be classified in this regime, according to the NMR data from Imai *et al.*[82] Furthermore, a crossover from Heisenberg to XY behavior induced in the spin dynamics by a very small anisotropy of the exchange interaction may explain the change in $\sigma(T)$ [or $\rho(T)$] at the characteristic temperature T_0. Monte Carlo calculations for undoped and doped systems give some support for this picture.

ACKNOWLEDGMENTS

The authors thank M. Maenhoudt and G. Jacob for sample preparation and E. Osquiguil and H. Adrian for useful discussions. This work has been supported by the Belgian Incentive Program on High Temperature Superconductors (SU.01), the Belgian Fund for Joint Basic Research (FKFO), the Belgian Fund for Scientific Research (NFWO), and inter-university attraction poles (IUAP) programmes.

[1] For a review, see N. P. Ong, in *Physical Properties of High Temperature Superconductors II*, edited by D. M. Ginsberg (World Scientific, Singapore, 1991), p. 459.
[2] For a review, see Y. Iye, in *Physical Properties of High Temperature Superconductors III*, edited by D. M. Ginsberg (World Scientific, Singapore, 1993), p. 285.
[3] K. Levin, J. H. Kim, J. P. Lu, and Q. Si, Physica C **175**, 449 (1991).
[4] P. W. Anderson and J. R. Schrieffer, Phys. Today **44**(6), 54 (1991).
[5] B. Wuyts, E. Osquiguil, M. Maenhoudt, S. Libbrecht, Z. X. Gao, and Y. Bruynseraede, Phys. Rev. B **47**, 5512 (1993).
[6] B. Wuyts, E. Osquiguil, M. Maenhoudt, S. Libbrecht, Z. X. Gao, and Y. Bruynseraede, Physica C **222**, 341 (1994).
[7] B. Wuyts, V. V. Moshchalkov, and Y. Bruynseraede, Phys. Rev. B **51**, 6115 (1995).
[8] T. Ito, K. Takenaka, and S. Uchida, Phys. Rev. Lett. **70**, 3995 (1993).
[9] A. Carrington, A. P. Mackenzie, C. T. Lin, and J. R. Cooper, Phys. Rev. Lett. **69**, 2855 (1992).
[10] H. Y. Hwang, B. Batlogg, H. Takagi, H. L. Kao, J. Kwo, R. J. Cava, J. J. Krajewski, and W. F. Peck, Jr., Phys. Rev. Lett. **72**, 2636 (1994).
[11] J. Rossat-Mignod, L. P. Regnault, P. Bourges, P. Burlet, C. Vettier, and J. Y. Henry, in *Selected Topics in Superconductivity*, edited by L. C. Gupta and M. S. Multani (World Scientific, Singapore, 1993), Vol. 1, p. 265.
[12] H. Alloul, in *High Temperature Superconductivity*, edited by D. P. Tunstall and W. Barford (Hilger, Bristol, 1991), p. 207.
[13] V. V. Moshchalkov, Solid State Commun. **86**, 715 (1993).
[14] B. Wuyts, Z. X. Gao, S. Libbrecht, M. Maenhoudt, E. Osquiguil, and Y. Bruynseraede, Physica C **203**, 235 (1992).
[15] E. Osquiguil, M. Maenhoudt, B. Wuyts, and Y. Bruynseraede, Appl. Phys. Lett. **60**, 1627 (1992).
[16] P. K. Gallagher, Adv. Ceram. Mater. **2**, 632 (1987).
[17] K. Takenaka, K. Mizuhashi, H. Takagi, and S. Uchida (unpublished).
[18] R. Beyers and T. M. Shaw, Solid State Phys. **42**, 135 (1989).
[19] M. Maenhoudt (private communication).
[20] M. Tetenbaum, L. A. Curtiss, B. Tani, B. Czech, and M. Blander, Physica C **158**, 371 (1989).
[21] B. W. Veal and A. P. Paulikas, Physica C **184**, 321 (1991).
[22] R. McCormack, D. de Fontaine, and G. Ceder, Phys. Rev. B **45**, 12 976 (1992).
[23] G. Uimin, Phys. Rev. B **50**, 9531 (1994).
[24] J. Harris, Y. F. Yan, and N. P. Ong, Phys. Rev. B **46**, 14 293 (1992).
[25] P. Xiong, G. Xiao, and X. D. Wu, Phys. Rev. B **47**, 5516 (1993).
[26] E. C. Jones, D. K. Christen, J. R. Thompson, R. Feenstra, S. Zhu, D. H. Lowndes, J. M. Phillips, M. P. Siegal, and J. D. Budai, Phys. Rev. B **47**, 8986 (1993).
[27] A. Carrington, D. J. C. Walker, A. P. Mackenzie, and J. R. Cooper, Phys. Rev. B **48**, 13 051 (1993).
[28] R. Decca, E. Osquiguil, F. de la Cruz, C. D'Ovidio, M. T. Malachevski, and D. Esparza, Solid State Commun. **69**, 355 (1989).
[29] H. Takagi, B. Batlogg, H. L. Kao, J. Kwo, R. J. Cava, J. J. Krajewski, and W. F. Peck, Jr., Phys. Rev. Lett. **69**, 2975 (1992).

[30] T. R. Chien, Z. Z. Wang, and N. P. Ong, Phys. Rev. Lett. **67**, 2088 (1991).
[31] W. Jiang, J. L. Peng, S. J. Hagen, and R. L. Greene, Phys. Rev. B **46**, 8694 (1992).
[32] J. I. Martin, B. Wuyts, M. Maenhoudt, E. Osquiguil, J. L. Vicent, V. V. Moshchalkov, and Y. Bruynseraede, Physica C (to be published).
[33] Z. Z. Wang, J. Clayhold, N. P. Ong, J. M. Tarascon, L. H. Greene, W. R. McKinnon, and G. W. Hull, Phys. Rev. B **36**, 7222 (1987).
[34] T. Penney, S. von Molnar, D. Kaiser, F. Holtzberg, and A. W. Kleinasser, Phys. Rev. B **38**, 2918 (1988).
[35] A. Davidson, P. Santhanam, A. Palevski, and M. J. Brady, Phys. Rev. B **38**, 2828 (1988).
[36] A. T. Fiory and G. S. Grader, Phys. Rev. B **38**, 9198 (1988).
[37] C. M. Hurd, *The Hall Effect in Metals and Alloys* (Plenum, New York, 1972).
[38] T. V. Ramakrishnan, P. Coleman, and P. W. Anderson, J. Magn. Magn. Mater. **47–48**, 493 (1985).
[39] A. Fert, J. Phys. F **3**, 2126 (1973).
[40] A. Fert and P. M. Levy, Phys. Rev. B **36**, 1907 (1987).
[41] Z. Z. Wang, T. R. Chien, N. P. Ong, J. M. Tarascon, and E. Wang, Phys. Rev. B **43**, 3020 (1991).
[42] K. Nakao, K. Hashimoto, K. Hayashi, Y. Enomoto, N. Koshizuka, and S. Tanaka, Physica C (to be published).
[43] G. Jakob, Ph.D. thesis, Technischen Hochschule, Darmstadt, 1993.
[44] P. F. Miceli, J. M. Tarascon, L. H. Greene, P. Barboux, F. J. Rotella, and J. D. Jorgensen, Phys. Rev. B **37**, 5932 (1988).
[45] J. Clayhold, S. Hagen, Z. Z. Wang, N. P. Ong, J. M. Tarascon, and P. Barboux, Phys. Rev. B **39**, 777 (1989).
[46] J. M. Tarascon, P. Barboux, P. F. Miceli, L. H. Greene, G. W. Hull, M. Eibschutz, and S. A. Sunshine, Phys. Rev. B **37**, 7458 (1988).
[47] L. Hofmann, K. Harl, and K. Samwer, Z. Phys. B **95**, 173 (1994).
[48] B. Bucher, P. Steiner, J. Karpinski, E. Kaldis, and P. Wachter, Phys. Rev. Lett. **70**, 2012 (1993).
[49] T. Nakano, M. Oda, C. Manabe, N. Momono, Y. Miura, and M. Ido, Phys. Rev. B **49**, 16 000 (1994).
[50] T. M. Rice, in *The Physics and Chemistry of Oxide Superconductors*, edited by Y. Iye and H. Yasuoka (Springer-Verlag, Berlin, 1992).
[51] V. V. Moshchalkov and N. B. Brandt, Sov. Phys. Usp. **29**, 725 (1986).
[52] H. Alloul, Phys. Rev. Lett. **63**, 689 (1989).
[53] M. Takigawa, A. P. Reyes, P. C. Hammel, J. D. Thompson, R. H. Heffner, Z. Fisk, and K. C. Ott, Phys. Rev. B **43**, 247 (1991).
[54] A. J. Millis, H. Monien, and D. Pines, Phys. Rev. B **42**, 167 (1992).
[55] T. Tanamoto, H. Kohno, and H. Fukuyama, J. Phys. Soc. Jpn. **63**, 2739 (1994).
[56] T. Nishikawa, J. Takeda, and M. Sato, J. Phys. Soc. Jpn. **62**, 2568 (1993).
[57] N. Y. Chen, V. C. Matijasevic, J. E. Mooij, and D. van der Marel, Phys. Rev. B **50**, 16 125 (1994).
[58] D. C. Johnston, Phys. Rev. Lett. **62**, 957 (1989).
[59] I. Tomeno, T. Machi, K. Tai, N. Koshizuka, S. Kambe, A. Hayashi, Y. Ueda, and H. Yasuoka, Phys. Rev. B **49**, 15 327 (1994).
[60] J. Karpinski, E. Kaldis, E. Jilek, S. Rusiecki, and B. Bucher, Nature **336**, 660 (1988).
[61] N. Nagaosa and P. A. Lee, Phys. Rev. B **45**, 966 (1992).
[62] N. Nagaosa and P. A. Lee, Phys. Rev. Lett. **64**, 2450 (1990).
[63] H. Zhang and H. Sato, Phys. Rev. Lett. **70**, 1697 (1993).
[64] L. P. Gor'kov, A. I. Larkin, and D. E. Khmelnitskii, JETP Lett. **30**, 228 (1979).
[65] S. Chakraverty, B. I. Halperin, and D. R. Nelson, Phys. Rev. B **39**, 2344 (1989).
[66] A. V. Chubukov, S. Sachdev, and J. Ye, Phys. Rev. B **49**, 11 919 (1994).
[67] For a review, see E. Manousakis, Rev. Mod. Phys. **63**, 1 (1991).
[68] A. Sokol and D. Pines, Phys. Rev. Lett. **71**, 2813 (1993).
[69] H.-Q. Ding, Phys. Rev. Lett. **68**, 1927 (1992).
[70] P. C. Hohenerg, Phys. Rev. **158**, 383 (1967).
[71] N. D. Mermin and H. Wagner, Phys. Rev. Lett. **17**, 1133 (1966).
[72] D. Reefman, Ph.D. thesis, Rijksuniversiteit, Leiden, 1993.
[73] L. J. de Jongh, Physica C **161**, 631 (1989).
[74] R. Micnas, J. Ranninger, and S. Robaszkiewicz, Rev. Mod. Phys. **62**, 113 (1990).
[75] A. Alexandrov and J. Ranninger, Phys. Rev. B **23**, 1796 (1981).
[76] J. M. Tranquada, P. M. Gehring, G. Shirane, S. Shamoto, and M. Sato, Phys. Rev. B **46**, 5561 (1992).
[77] V. V. Moshchalkov, Physica C **156**, 473 (1988).
[78] V. V. Moshchalkov, Physica B **163**, 59 (1990).
[79] J. Genossur, B. Fisher, and J. Ashkenazi, Physica C **162–164**, 1015 (1989).
[80] K. Gofron, J. C. Campuzano, A. A. Abrikosov, M. Lindroos, A. Bansil, H. Ding, D. Koelling, and B. Dabrowski, Phys. Rev. Lett. **73**, 3302 (1994).
[81] D. M. King, Z.-X. Shen, D. S. Dessau, D. S. Marshall, C. H. Park, W. E. Spicer, J. L. Peng, Z. Y. Li, and R. L. Greene, Phys. Rev. Lett. **73**, 3298 (1994).
[82] T. Imai, C. P. Slichter, K. Yoshimura, M. Katoh, and K. Kosuge, Physica B **197**, 601 (1994).